

APPLICATION
FOR
UNITED STATES LETTERS PATENT

TITLE: RECTANGULAR SUPRAMOLECULES

APPLICANT: KUANG-LIEH LU, MANIMARAN BALA,
T. RAJENDRAN, YI-LONG LU, GENE-HSIANG LEE
AND SHIE-MING PENG

CERTIFICATE OF MAILING BY EXPRESS MAIL

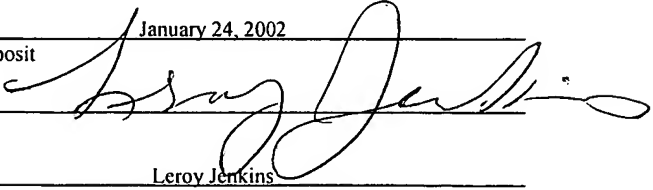
Express Mail Label No. EL932076005US

I hereby certify under 37 CFR §1.10 that this correspondence is being deposited with the United States Postal Service as Express Mail Post Office to Addressee with sufficient postage on the date indicated below and is addressed to the Commissioner for Patents, Washington, D.C. 20231.

Date of Deposit

January 24, 2002

Signature



Leroy Jenkins

Typed or Printed Name of Person Signing Certificate

Rectangular Supramolecules

BACKGROUND

Transition-metal-based supramolecules have been extensively explored in recent years. These supramolecules, which can be squares, helices, boxes, cages, or rectangles, are of particular interest due to their applications in host-guest interactions, molecular recognition, and as molecular sensors. See, e.g., Lehn, *Supramolecular Chemistry: Concepts and Perspectives*; VCH: Weinheim, 1995; Leininger, *et al.* (2000) *Chem. Rev.* 100: 853; Swiegers & Malefetse (2000) *Chem. Rev.* 100: 3483; Caulder & Raymond (1999) *J. Chem. Soc., Dalton Trans.* 1185; MacGillivray & Atwood (1999). *Angew. Chem. Int. Ed.* 38: 1018; Constable & Schofield (1998) *Chem. Commun.* 403; Fujita (1999) *Acc. Chem. Res.* 32: 53; Fujita (1998) *Chem. Soc. Rev.* 27: 417; Imamura & Fukushima (2000) *Coord. Chem. Rev.* 198: 133; Dixon *et al.* (2000) *Inorg. Chem.* 39: 3432; and Sun & Lees (2000) *J. Am. Chem. Soc.* 122: 8956.

It has been established that a transition-metal-based supramolecule offers the feasibility of host-guest interactions and molecular recognition phenomena based on Coulombic or hydrophobic binding, where the binding affinity is highly dependent on the cavity size inside the supramolecule (*Sun & Lee supra*). The cavity may function as a catalytic microreactor. The supramolecule has been known to possess a net charge and require a counterion within its cavity. The counterion affects the cavity size as well as molecular sensing properties of the supramolecule. It is desirable to design and prepare a supramolecule that is neutral.

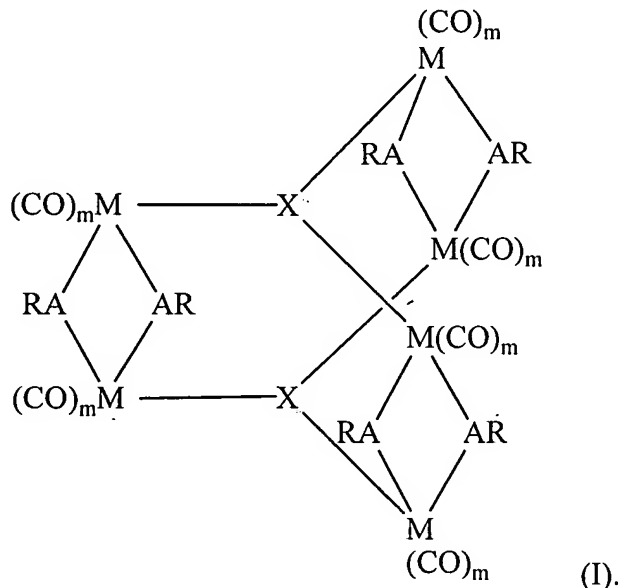
In addition, incorporation of photo-active centers into a transition-metal-based supramolecule is also desirable in molecular sensing technology. This application provides an alternative to the detection of guest inclusion based on photoluminescence characteristics. For example, if a supramolecule is luminescent, it can be used as a tool in lieu of ^1H NMR spectroscopy for detecting guest inclusion and studying electronic excited state reactivity and possible manipulation of reactivity by encapsulated guests. See, e.g., Slone *et al.* (1998) *Coord. Chem. Rev.* 171: 221; De Silva *et al.* (1997) *Chem. Rev.* 97: 1515; and Keefe *et al.* (2000) *Coord. Chem. Rev.* 205: 201.

There is a need for designing and preparing a transition-metal-based supramolecule that is neutral and luminescent.

SUMMARY

The invention is based on the discovery of four new classes of supramolecules having prismatic and rectangular structures. The new supramolecules are neutral and luminescent, and can be prepared by a one-pot synthesis method.

In one aspect, this invention features a prismatic supramolecule having structure (I):

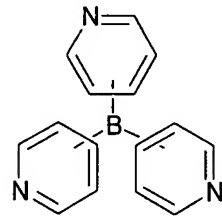


M is a transition metal atom that is rhenium (Re), manganese (Mn), chromium (Cr), molybdenum (Mo), tungsten (W), iron (Fe), ruthenium (Ru), or osmium (Os); X is a nitrogen-based tridentate ligand; A is O, S, Se, or Te; R is C₁-C₁₆ alkyl, (CH₂)_n-aryl, or (CH₂)_n-aryl-(O-C₁-C₁₆ alkyl)_p, in which n is 0-15, p is 1-3; and m is 1, 2, 3, 4, or 5. Other transition metal atoms may be utilized in accordance with the present invention as long as they, together with ligands, can form a coordination complex having the prismatic structures.

As used herein, the term "prismatic" refers to a compound having six transition metal atoms connected in a prismatic cage-like geometry. Each of the metal atoms occupies one corner of the prism and is bonded to one nitrogen of a nitrogen-based tridentate ligand, i.e., X in structure (I).

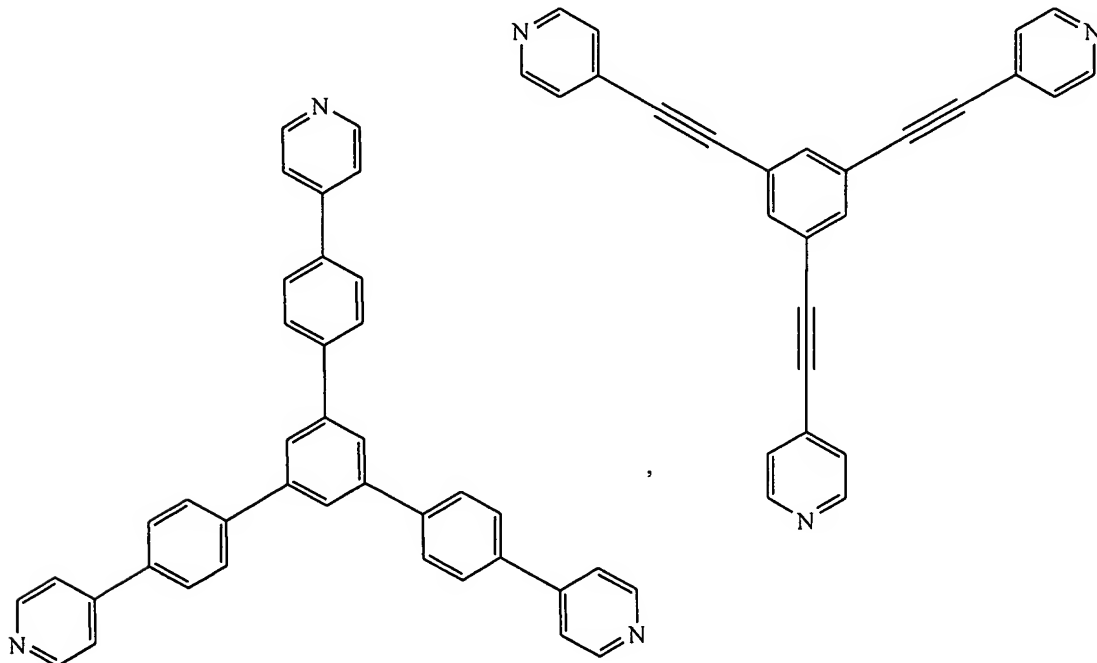
A “nitrogen-based tridentate ligand” refers to a ligand that is bonded to three transition metal atoms, and includes one or more heterocyclic or heteroaryl groups (e.g., triazine, pyrazole, imidazole, or pyridine) having one or more nitrogen atoms.

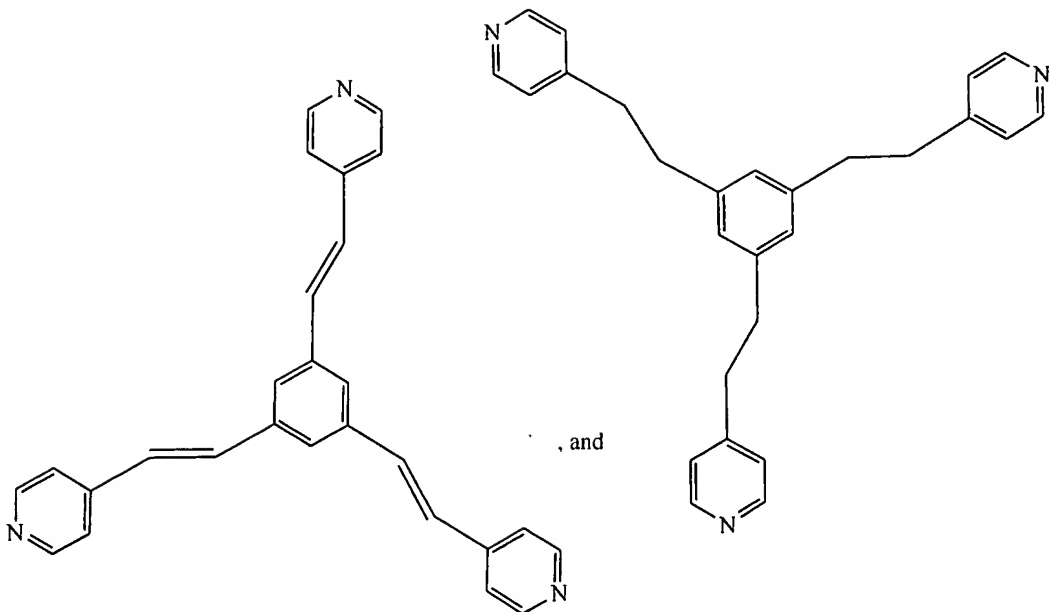
Referring to structure (I), a subset of prismatic supramolecules of this invention are those in which M is Re; m is 3; R is C₁~C₁₆ straight chain alkyl; A is O; and X is triazine or a ligand of the formula:



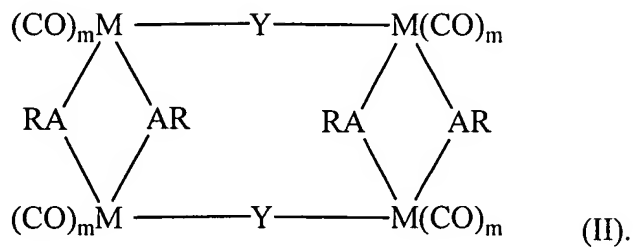
In the above formula, B is alkyl, alkenyl, alkynyl, cyclyl, heterocyclyl, aryl, or heteroaryl (e.g., 1,3,5-triazine); further, the three rings can be fused together with B (not shown), e.g., triaza-triphenylene or triaza-trinaphthylene. An example of X is 2,4,6-tri-4-pyridyl-1,3,5-triazine (referred to hereinafter as “tpt”).

Additional examples of X are shown below:





In another aspect, this invention features a rectangular supramolecule having structure (II):

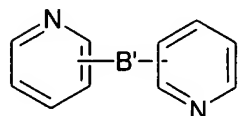


- 5 M is a transition metal atom that is Re, Mn, Cr, Mo, W, Fe, Ru, or Os; Y is a nitrogen-based didentate ligand; A is O, S, Se, or Te; R is C₃~C₁₆ alkyl, (CH₂)_n-aryl, or (CH₂)_n-aryl-(O-C₁~C₁₆ alkyl)_p, in which n is 0-15, p is 1-3; and m is 1, 2, 3, 4, or 5.

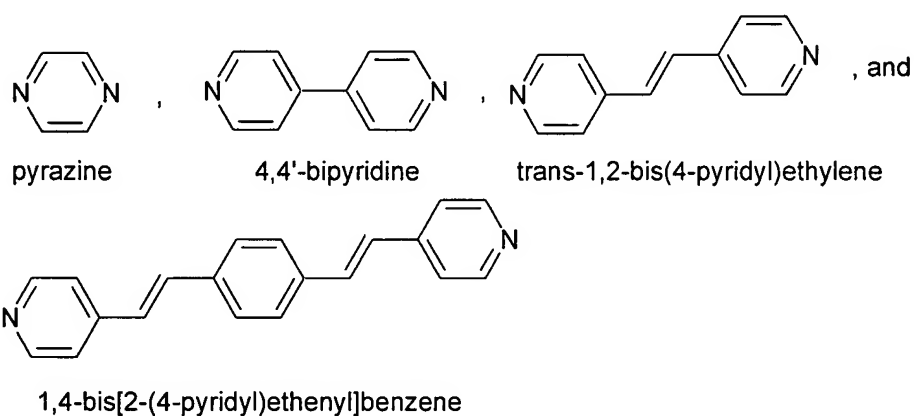
10 As used herein, the term “rectangular” refers to a compound having four transition metal atoms connected in a rectangular geometry. Each of the transition metal atoms occupies one corner of the rectangle, and is bonded to one nitrogen atom of a nitrogen-based didentate ligand.

A “nitrogen-based didentate ligand” refers to a ligand that is bonded to two transition metal atoms, and includes one or more heterocyclic or heteroaryl groups having one or more nitrogen atoms.

Referring to structure (II), a subset of rectangular supramolecules of this invention are those in which M is Re; m can be 3; R is C₃~C₁₆ straight chain alkyl; A is O; and Y is diazine or a ligand of the formula:



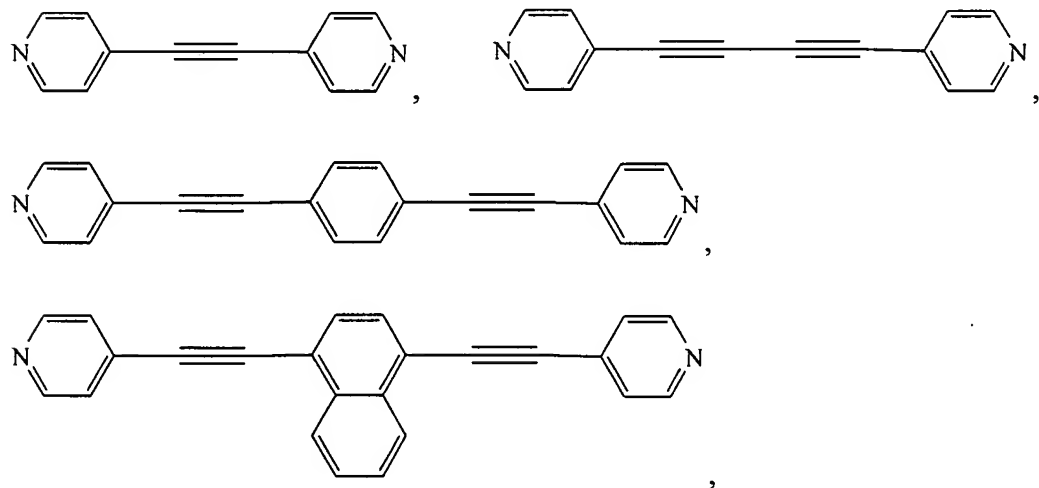
- 5 B' is a bond, alkyl, alkenyl, alkynyl, cyclyl, heterocyclyl, aryl, or heteroaryl; further, the two rings can be fused together with B (not shown), e.g., diaza-anthracene or 1,6-Dihydro-benzo[1,2-m][3,8]phenanthroline. Examples of Y include

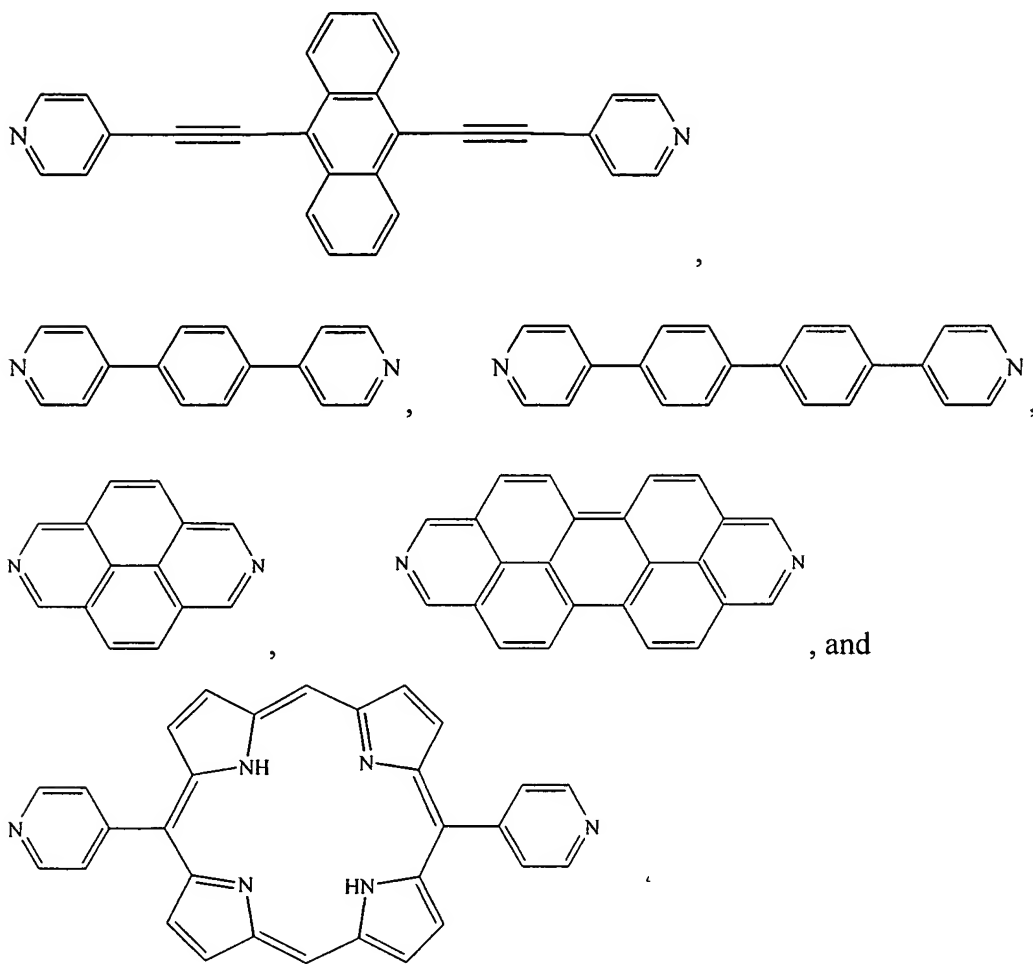


(referred to hereinafter as "pz," "bpy," "bpe," or "bpeb," respectively).

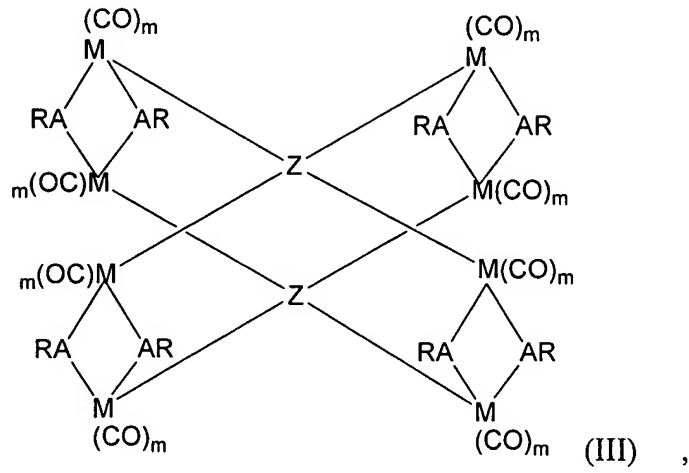
10

Additional examples of Y are shown below:





5 In further another aspect, this invention features a tetragonal prismatic supramolecule having structure (III):

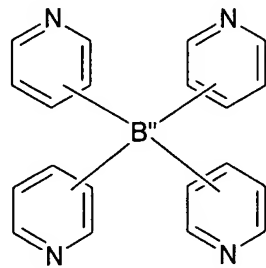


M is Re, Mn, Cr, Mo, W, Fe, Ru, or Os; Z is a nitrogen-based tetradentate ligand; A is O, S, Se, or Te; R is C₁~C₁₆ alkyl, (CH₂)_n-aryl, or (CH₂)_n-aryl-(O-C₁~C₁₆ alkyl)_p, in which n is 0-15, p is 1-3; and m is 1, 2, 3, 4, or 5.

As used herein, the term “tetragonal prismatic” refers to a compound having eight transition metal atoms connected in a prismatic cage-like geometry. Each of the metal atoms occupies one corner of the prism and is bonded to one nitrogen of a nitrogen-based tetradentate ligand, i.e., Z in structure (III).

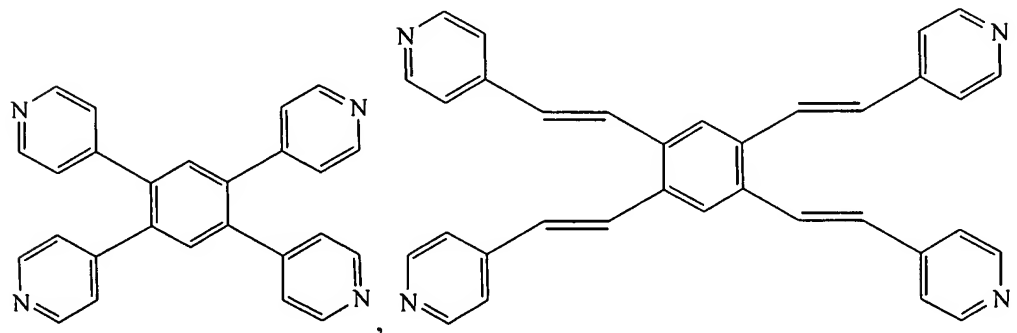
A “nitrogen-based tetradentate ligand” refers to a ligand that is bonded to four transition metal atoms, and includes one or more heterocyclic or heteroaryl groups (e.g., triazine, pyrazole, imidazole, or pyridine) having one or more nitrogen atoms.

Referring to structure (III), a subset of tetragonal prismatic supramolecules of this invention are those in which M is Re; m is 3; R is C₁~C₁₆ straight chain alkyl; A is O; and Z is tetrazine or a ligand of the formula:



In the above formula, B'' is alkyl, alkenyl, alkynyl, cyclyl, heterocyclyl, aryl, or heteroaryl; further, the four rings can be fused together with B'' (not shown), e.g., tetraaza-tetraphenylenes. An example of Z is 1,2,4,5-tetraethynyl(4-pyridyl)benzene (referred to hereinafter as “tpeb”).

Additional examples of Z are shown below.



The image shows two chemical structures side-by-side. Both structures consist of a six-membered pyridine ring with a methyl group (a black triangle) attached to one of the ring carbons. In the left structure, the methyl group is at the 2-position relative to the nitrogen atom (which is at the top). In the right structure, the methyl group is at the 4-position relative to the nitrogen atom.

The chemical structure shows a central 4,4'-biphenylene group. Attached to each biphenylene ring are two phenyl groups, one at the para position and one at the meta position relative to the biphenylene linkage. Each phenyl group is further substituted with a 4-pyridylmethyl group.

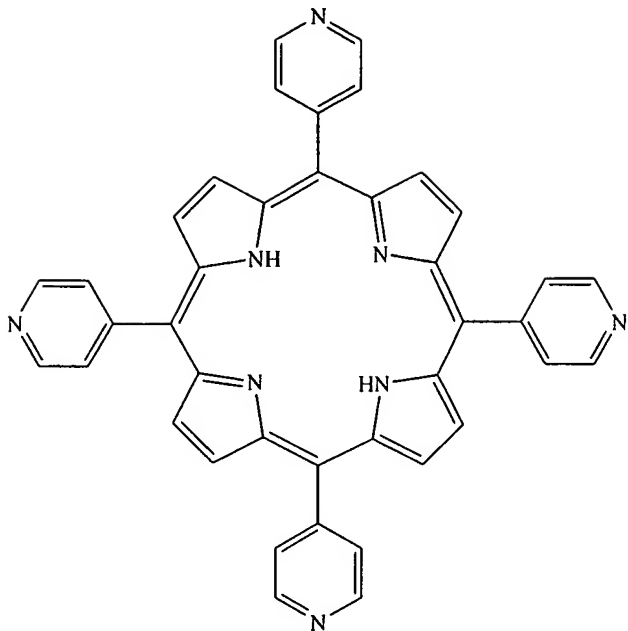
The image shows two chemical structures side-by-side. The left structure is 2-methylpyridine, featuring a six-membered pyridine ring with a methyl group (a black circle) attached to the second carbon atom. The right structure is 4-methylpyridine, featuring a six-membered pyridine ring with a methyl group attached to the fourth carbon atom.

The chemical structure shows a central benzene ring connected to two 4-phenylbut-1-enyl groups via methylene bridges.

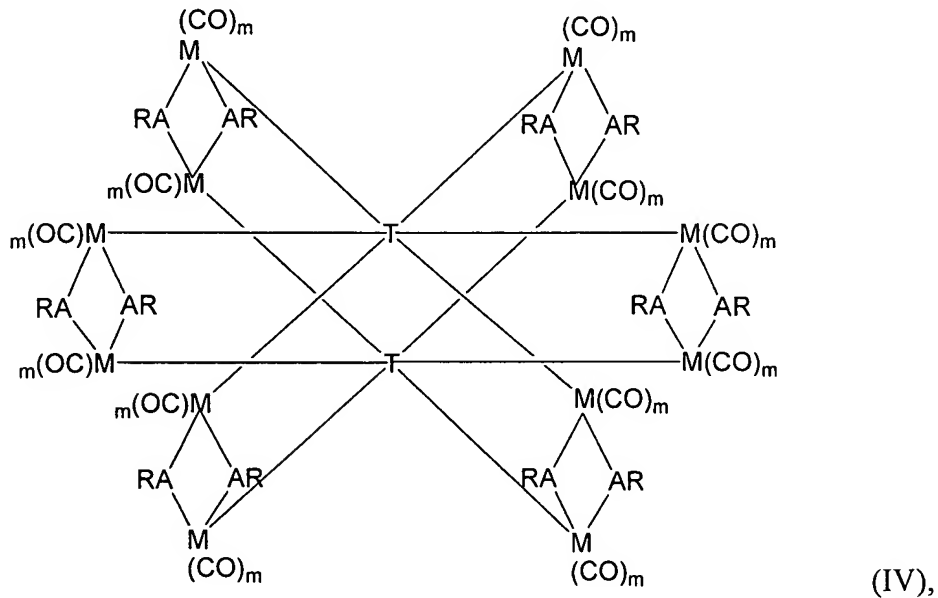
The chemical structure shows a 1,4-diphenyl-1,3-butadiene molecule. It consists of a central carbon atom bonded to two phenyl groups (benzene rings) at the 1 and 4 positions of a 1,3-butadiene chain.

The chemical structure shows a pyridine ring with an ethynyl group (-C≡C-) attached at the 4-position.

, and



In still another aspect, this invention features a hexagonal prismatic supramolecule having structure (IV):



5. M is Re, Mn, Cr, Mo, W, Fe, Ru, or Os; T is a nitrogen-based hexadentate ligand; A is O, S, Se, or Te; R is C₁~C₁₆ alkyl, (CH₂)_n-aryl, or (CH₂)_n-aryl-(O-C₁~C₁₆ alkyl)_p, in which n is 0-15, p is 1-3; and m is 1, 2, 3, 4, or 5.

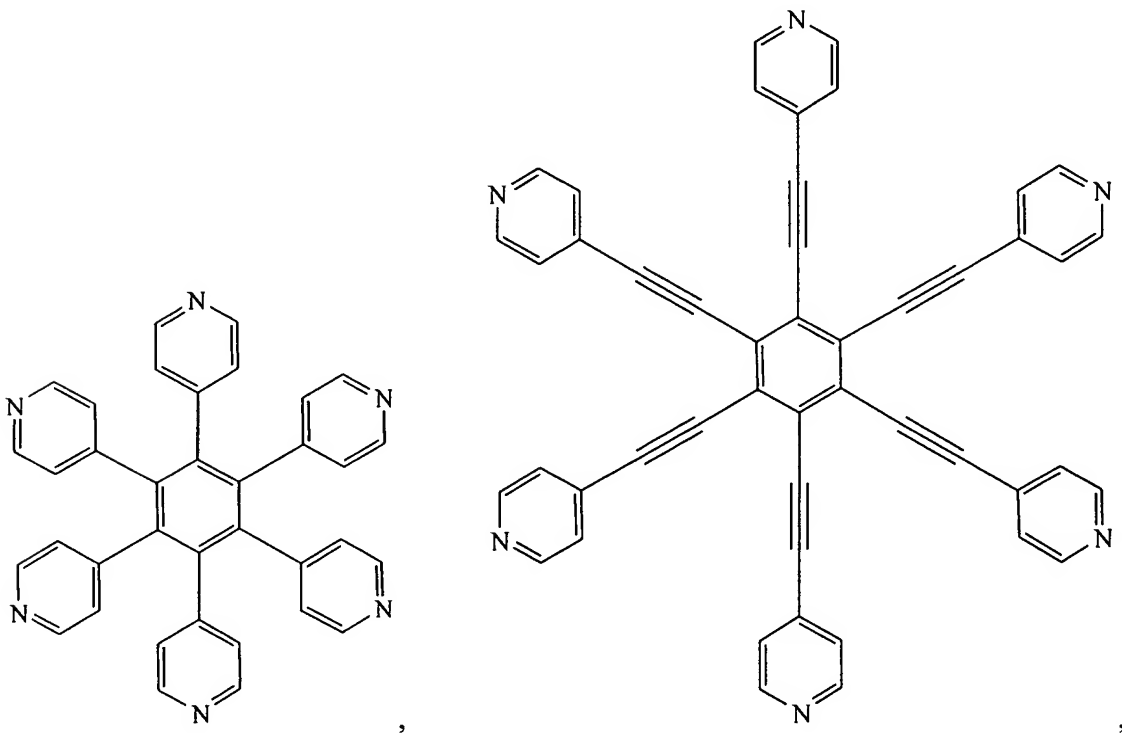
As used herein, the term "hexagonal prismatic" refers to a compound having twelve transition metal atoms connected in a prismatic cage-like geometry. Each of the metal atoms

occupies one corner of the prism and is bonded to one nitrogen of a nitrogen-based hexadentate ligand, i.e., T in structure (IV).

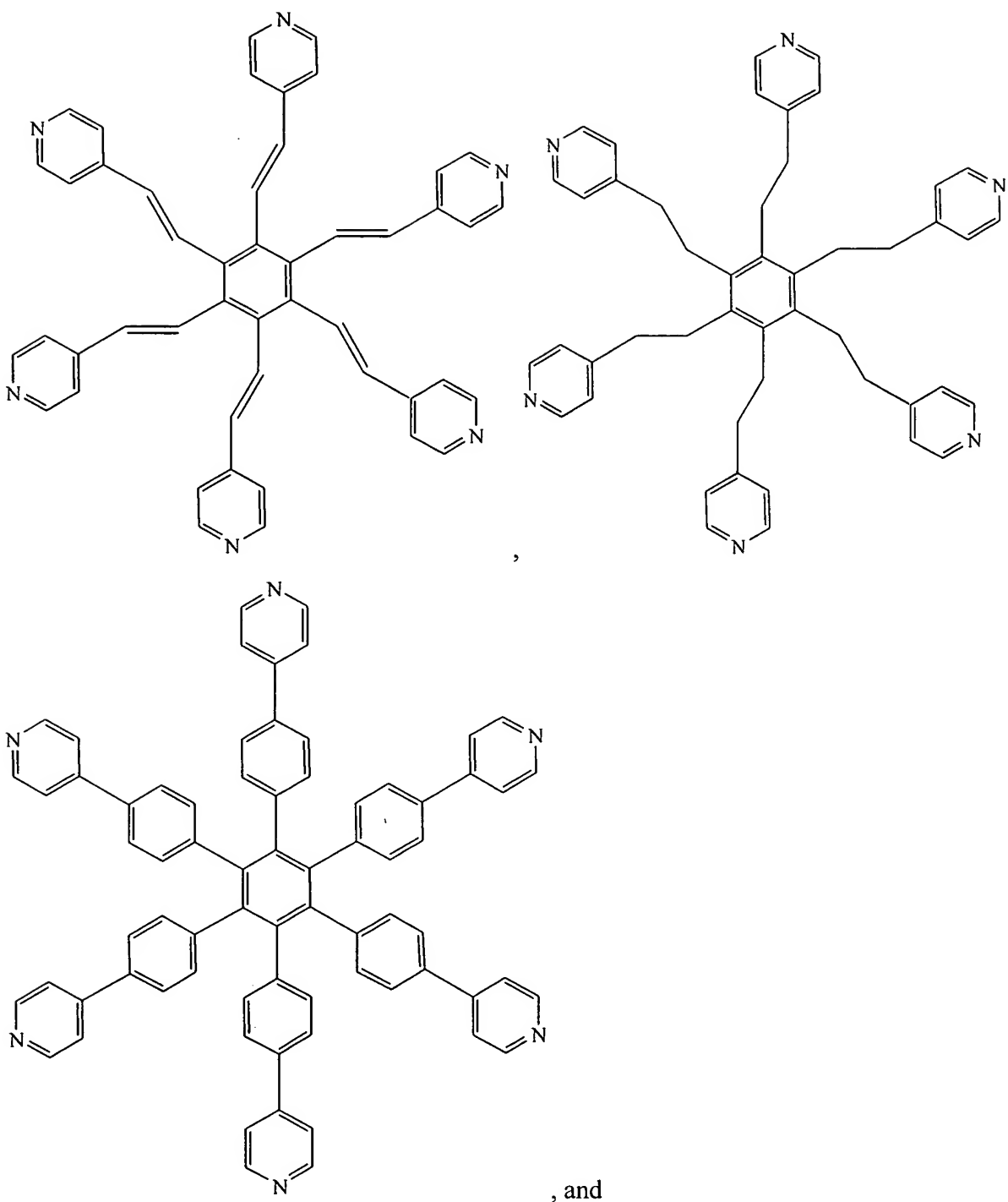
A “nitrogen-based hexadentate ligand” refers to a ligand that is bonded to six transition metal atoms, and includes one or more heterocyclic or heteroaryl groups (e.g., triazine, pyrazole, imidazole, or pyridine) having one or more nitrogen atoms.

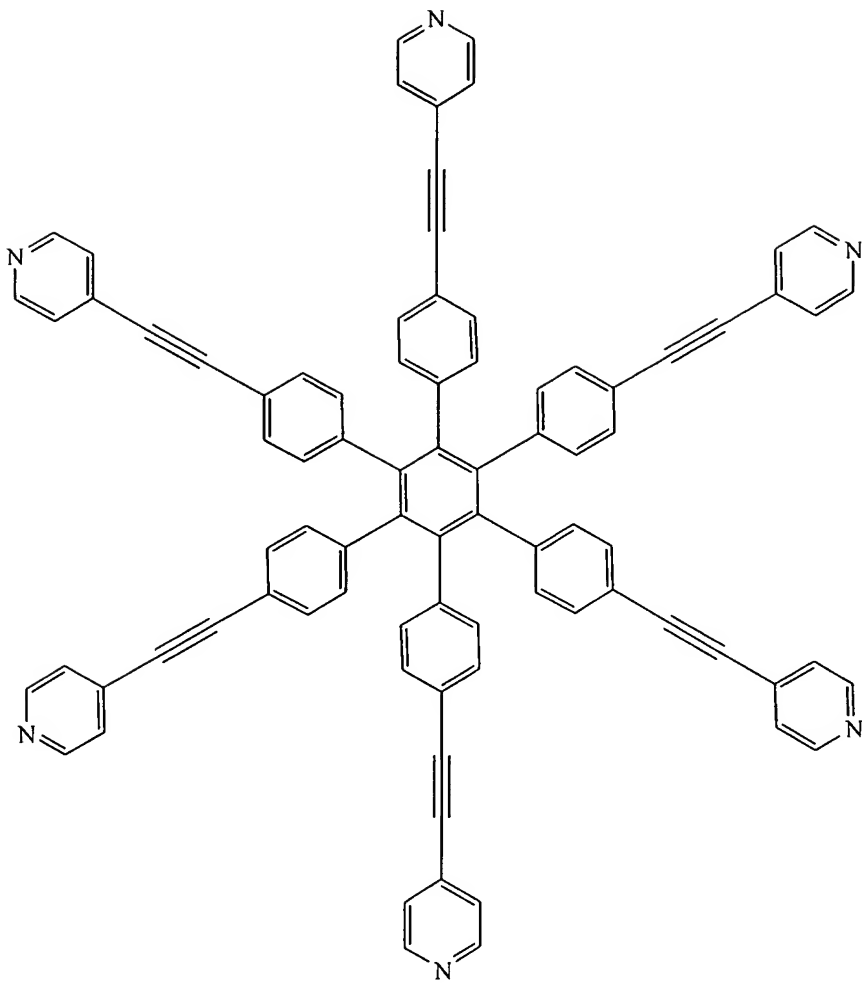
Referring to structure (IV), a subset of hexagonal prismatic supramolecules of this invention are those in which M is Re; m is 3; R is C₁~C₁₆ straight chain alkyl; and A is O.

Examples of T are shown below.



0007029-042402





Alkyl, alkenyl, alkynyl, cyclyl, heterocyclyl, aryl, or heteroaryl (e.g., triazine, diazine, or pyridine) mentioned above include both substituted and unsubstituted moieties. As used herein, alkyl, alkenyl, alkynyl are straight or branched hydrocarbon chains. The term "substituted" refers to one or more substituents (which may be the same or different), each in replace of a hydrogen atom. Examples of substituents include, but are not limited to, halogen, hydroxyl, amino, cyano, nitro, C₁~C₆ alkyl, C₂~C₆ alkenyl, C₂~C₆ alkynyl, C₁~C₆ alkoxy, aryl, heteroaryl, and heterocyclyl, wherein alkyl, alkenyl, alkoxy, aryl, heteroaryl and heterocyclyl are optionally substituted with C₁~C₆ alkyl, C₂~C₆ alkenyl, C₂~C₆ alkynyl, aryl, heteroaryl, halogen, hydroxyl, amino, cyano, or nitro. The term "aryl" refers to a hydrocarbon ring system having at least one aromatic ring. Examples of aryl moieties include, but are not limited to, phenyl, naphthyl, and pyrenyl. The term "heteroaryl" refers to a hydrocarbon ring system having at least one aromatic ring which contains at least one

201906250000

heteroatom such as O, N, or S. Examples of heteroaryl moieties include, but are not limited to, pyridyl, carbazolyl, and indolyl.

Set forth below are exemplary compounds of this invention:

Compounds 1-3 having prismatic structure (I), in which M is Re; m is 3; and A is O;

5 Compound 1: R = C₄H₉; X = tpt;

Compound 2: R = C₈H₁₇; X = tpt; and

Compound 3: R = C₁₂H₂₅; X = tpt;

Compounds 4-12 having rectangular structure (II), in which M is Re; m is 3; and A is O;

Compound 4: R = (CH₂)₃CH₃; Y = pz;

10 Compound 5: R = (CH₂)₇CH₃; Y = pz;

Compound 6: R = (CH₂)₃CH₃; Y = bpe;

Compound 7: R = (CH₂)₇CH₃; Y = bpe;

Compound 8: R = (CH₂)₃CH₃; Y = bpeb;

Compound 9: R = (CH₂)₃CH₃; Y = pz;

15 Compound 10: R = (CH₂)₃CH₃; Y = bpy;

Compound 11: R = (CH₂)₇CH₃; Y = bpy; and

Compound 12: R = (CH₂)₁₁CH₃; Y = bpy.

Compounds 13-15 having tetragonal prismatic structure (III), in which M is Re; m is 3; and A is O;

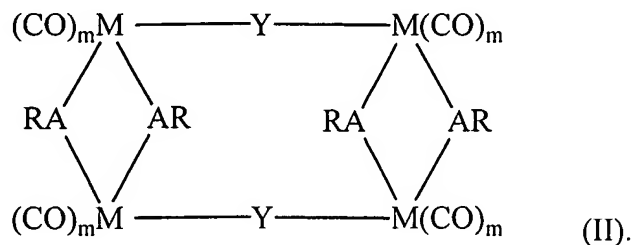
20 Compound 13: R = C₈H₁₇; Z = tpeb;

Compound 14: R = C₁₂H₂₅; X = tpeb; and

Compound 15: R = C₇H₇; X = tpeb.

In still another aspect, this invention features a one-pot synthesis method for making a prismatic supramolecule of this invention. The method includes reacting M(CO)_{m+2} with a nitrogen-based tridentate ligand in the presence of an RAH (see structure (I), e.g., a C₁-C₁₆ aliphatic alcohol) at an elevated temperature to form a thermodynamically stable prismatic supramolecule. When RAH is an alcohol, the reaction can be carried out using a solvothermal approach or a refluxing approach. In the solvothermal approach, the alcohol serves as the only solvent and also as one reactant. In the refluxing approach, one or more other organic solvents can be used together with the alcohol.

In further another aspect, this invention features a one-pot synthesis method for making a rectangular supramolecule having structure (II):

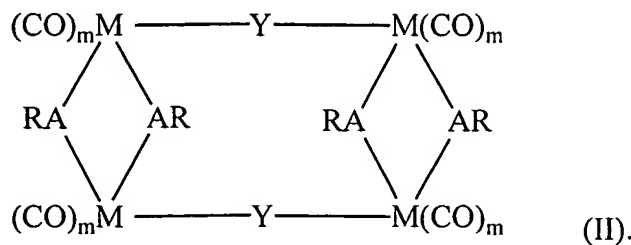


M is Re, Mn, Cr, Mo, W, Fe, Ru, or Os; Y is a nitrogen-based didentate ligand; A is O, S, Se, or Te; R is C₁~C₁₆ alkyl or (CH₂)_n-aryl, in which n is 0-15; and m is 1, 2, 3, 4, or 5. This method includes reacting M(CO)_{m+2} with a nitrogen-based didentate ligand in the presence of an RAH at an elevated temperature to form the rectangular supramolecule.

Additionally, this invention features a one-pot synthesis method for making a tetragonal prismatic supramolecule of this invention. The method includes reacting M(CO)_{m+2} with a nitrogen-based tetradentate ligand in the presence of an RAH (see structure (III), e.g., a C₁~C₁₆ aliphatic alcohol) at an elevated temperature to form a thermodynamically stable tetragonal prismatic supramolecule.

Further, this invention also feature a one-pot synthesis method for making a hexagonal prismatic supramolecule of this invention. The method includes reacting M(CO)_{m+2} with a nitrogen-based hexadentate ligand in the presence of an RAH (see structure (IV), e.g., a C₁~C₁₆ aliphatic alcohol) at an elevated temperature to form a thermodynamically stable hexagonal prismatic supramolecule.

Also within the scope of this invention is a composition for emitting luminescence at room temperature. The composition can include an aqueous solution (e.g., a mixture of THF and H₂O, a mixture of CH₃CN and H₂O, a mixture of CH₃COCH₃ and H₂O, a mixture of CH₃OH and H₂O, or a mixture of CH₃CH₂OH and H₂O) and a rectangular supramolecule having structure (II):



M is Re, Mn, Cr, Mo, W, Fe, Ru, or Os; Y is a nitrogen-containing didentate ligand; A is O, S, Se, or Te; R is C₁~C₁₆ alkyl or (CH₂)_n-aryl, in which n is 0-15; and m is 1, 2, 3, 4, or 5. Preferably, R is C₈~C₁₂ straight chain alkyl. Alternatively, the composition can include a prismatic supramolecule of this invention and an aqueous solution. Further, the composition
5 can include a tetragonal prismatic supramolecule of this invention and a solution, such as pyridine, methyl phenyl sulfide, or an aqueous solution described above.

The invention provides several advantages. For example, the four new classes of supramolecules (i.e., having prismatic and rectangular structures) described above are neutral, air and moisture stable, and soluble in organic and polar solvents. In addition, the
10 supramolecules exhibit luminescence.

Other advantages, features, and objects of the invention will be apparent from the description and from the claims.

DETAILED DESCRIPTION

The invention covers four new classes of supramolecules having prismatic and rectangular structures. Such supramolecules described in the "Summary" section can be prepared by methods also within the scope of this invention. More specifically, one can react M(CO)_{m+2} (M is Re, Mn, Cr, Mo, W, Fe, Ru, or Os; and m is any single number between 1-5) with a nitrogen-based di-, tri-, tetra-, or hexa-dentate ligand in the presence of an RAH (see structures (I) (II), (III), and (IV) above, e.g., a C₁~C₁₆ aliphatic alcohol) at an elevated
15 temperature to form a supramolecule. For example, when the RAH is an alcohol, the reaction can be carried out using a solvothermal approach, in which the alcohol serves as the only solvent and also as a reactant. In this approach, the reaction temperature is higher than the boiling point of the alcohol. The reaction proceeds until the most thermodynamically stable supramolecule forms. Unexpectedly, this reaction affords supramolecule crystals of
20 high quality, such as X-ray quality crystals. If necessary, the supramolecule can be further purified by flash column chromatography, high performance liquid chromatography, or re-crystallization. One can design and prepare a supramolecule having desired structures and physical properties (e.g., prismatic cages, rectangles, cavity sizes, or hydrophobicities) by
25 adjusting the experimental conditions and choosing an appropriate ligand.

The supramolecules described above are useful in molecular sensing technology. Many of the previously reported supramolecules are charged, with counterions trapped inside the cavities of the charged supramolecules. The trapped counterions interfere with host-guest interactions or affect molecular sensing properties. In contrast, the supramolecules of this invention are neutral and have no counterions inside their cavities. Additionally, such supramolecules can obtain various di-, tri-, tetra-, or hexa-dentate ligands and therefore, possess diverse size cavities, making them suitable as hosts for a variety of guest molecules in the solid state as well as in solution. Thus, the supramolecules in accordance with the present invention may be used to detect and measure the inclusion of guest molecules of varying sizes, including aromatic hydrocarbons (e.g., anthracene, p-xylene, pyrene, phenanthrene, triphenylene, chrysene, benzopyrene, dicyanobenzene, or benzanthracene), nitro compounds (e.g., nitrobenzene, m-dinitrobenzene, nitrotoluene, 2,4-dinitrotoluene, or 2,6-dinitrotoluene), amines (e.g., tetramethylphenylenediamine, tetramethylbenzidine, p-anisidine, or diphenylamine), quinines (e.g., toluiquinone, benzoquinone, naphthaquinone, or anthraquinone), and some metal salts (e.g., AgNO₃, Zn(NO₃)₂, Co(NO₃)₂, or Cd(NO₃)₂) or complexes (e.g., [Ru(bpy)₃]Cl₂).

The detection and measurement can be based on the supramolecules' electrochemical properties (e.g., showing changes in redox potential values), photophysical/photochemical properties (e.g., showing changes in emission or absorption spectra), or solvatochromism (e.g., showing visible color changes depending on the polarity of a solvent). The NMR technique is one conventional method for detecting and measuring host-guest interactions.

More specifically, the rectangular or prismatic supramolecules described above exhibit luminescence in a solution, and therefore are useful in molecular sensors for detecting and measuring the inclusion of target molecules based on photoluminescence characteristics. The exhibited luminescence of these supramolecules is unexpectedly bright when the supramolecules are in an aqueous solution. The brightness in an aqueous solution may be due to self-aggregation of the supramolecules, and can be used effectively in sensor applications. For example, the rectangular supramolecules in an aqueous solution provide a more sensitive spectroscopic detection technique than the conventional NMR method for monitoring host-guest interactions.

The specific examples below are to be construed as merely illustrative, and not limitative of the remainder of the disclosure in any way whatsoever. Without further elaboration, it is believed that one skilled in the art can, based on the description herein, utilize the present invention to its fullest extent. All publications cited herein are hereby incorporated by reference in their entirety.

Example 1. Synthesis of Compounds 1-3 having prismatic structures

A suspension consisting of a mixture of $\text{Re}_2(\text{CO})_{10}$ (98 mg, 0.15 mmol) and tpt (32 mg, 0.10 mmol) in 10 mL 1-butanol in a 30 mL Teflon flask was placed in a steel bomb. The bomb was placed in an oven maintained at 180 °C for 48 h and then cooled to 25 °C. Good quality maroon colored single crystals of Compound 1 were obtained. The crystals were separated by filtration and washed with 1-butanol. Compounds 2 and 3 were also synthesized by adopting a similar procedure. The solvent from the reaction mixture was removed by vacuum distillation and the residue was redissolved in CH_2Cl_2 and passed through short silica gel column to get the pure products of Compounds 2 and 3. (Yield: Compound 1, 109 mg, 81 %; Compound 2, 124 mg, 82 %; Compound 3, 142 mg, 85 %)

[$\{\{\text{CO}\}_3\text{Re}(\mu_2-\text{OC}_4\text{H}_9)_2\text{Re}(\text{CO})_3\}_3(\mu_3\text{-tpt})_2$] (Compound 1): Elemental analysis: Calcd: C, 34.89; H, 2.93; N, 6.26; found: C, 35.06; H, 2.94; N, 6.40; Crystal data ($\text{C}_{78}\text{H}_{78}\text{N}_{12}\text{O}_{24}\text{Re}_6$): Crystal dimensions $0.20 \times 0.10 \times 0.03$ mm, rhombohedral, space group $R\bar{3}c$, $a = b = 23.4486(9)$, $c = 27.6604(11)$ Å, $\alpha = \beta = 90^\circ$, $\gamma = 120^\circ$, $V = 13171.1(9)$ Å³, $Z = 6$, $T = 150(1)$ K, $\rho_{\text{calcd}} = 2.031$ Mg/m³, $\mu = 8.316$ mm⁻¹, 9628 total reflections, 2539 independent reflections which were used in refinement. The structure was solved to $R1 = 0.0865$ and $wR2 = 0.1166$.

[$\{\{\text{CO}\}_3\text{Re}(\mu_2-\text{OC}_8\text{H}_{17})_2\text{Re}(\text{CO})_3\}_3(\mu_3\text{-tpt})_2$] (Compound 2): IR (CH_2Cl_2): ν_{CO} 2022 (s), 2009 (m), 1913 (m), 1890 (vs) cm⁻¹; ¹H NMR (300 MHz, CDCl_3): δ 8.72 (d, ³J = 6.5 Hz, 12 H, H³), 8.24 (d, 12 H, H²), 4.43 (t, ³J = 8.0 Hz, 12 H), 2.15 (m, 12 H), 1.49 (m, 36 H), 1.25 (m, 24 H), 0.94 (t, ³J = 6.7 Hz, 18 H); ¹³C NMR (75 MHz; CDCl_3): δ = 197.2 (s, CO), 170.1 (C, triazine), 153.5 (C³), 142.2 (C¹), 123.2 (C²), 82.9 (CH₂), 34.2 (CH₂), 31.9 (CH₂), 29.7 (CH₂), 29.4 (CH₂), 25.3 (CH₂), 22.7 (CH₂), 14.2 (CH₃); UV-Vis (CH_2Cl_2): λ_{max} [nm]

(MLCT) 488, λ_{\max} [nm] (LIG) 243; Elemental analysis: Calcd: C, 40.55; H, 4.20; N, 5.56; found: C, 40.56; H, 4.23; N, 5.53; Mass (FAB, ^{187}Re): m/z = 3024 (M^+).

[{(CO)₃Re(μ_2 -OC₁₂H₂₅)₂Re(CO)₃}₃(μ_3 -tpt)₂] (Compound 3): IR (CH₂Cl₂): ν_{CO} 2022 (s), 2009 (m), 1913 (m), 1890 (vs) cm⁻¹; ¹H NMR (300 MHz, CDCl₃): δ = 8.72 (d, ³J = 6.5 Hz, 12 H, H³), 8.24 (d, 12 H, H²), 4.42 (t, ³J = 8.0, 12 H), 2.15 (m, 12 H), 1.48 (m, 24 H), 1.29 (m, 84 H), 0.88 (t, ³J = 6.2 Hz, 18 H); ¹³C NMR (75 MHz; CDCl₃): δ = 197.2, 197.1 (s, 1:2 CO), 170.1 (C, triazine), 153.5 (C³), 142.1 (C¹), 123.2 (C²), 82.8 (CH₂), 34.1 (CH₂), 31.9 (CH₂), 31.5 (CH₂), 29.7 (2 CH₂), 29.6 (2 CH₂), 29.3 (CH₂), 25.2 (CH₂), 22.7 (CH₂), 14.1 (CH₃); UV-Vis (CH₂Cl₂): λ_{\max} [nm] (MLCT) 488, λ_{\max} [nm] (LIG) 242; Elemental analysis: Calcd: C, 44.99; H, 5.22; N, 5.00; found: C, 45.52; H, 5.30; N, 4.92; Mass (FAB, ^{187}Re): m/z = 3360 (M^+).

The ORTEP drawing of Compound 1 revealed a prismatic cage architecture, where two planar tpt ligands coordinated to six rhenium atoms, which were connected by six butoxo bridges, thereby forming a triangular prismatic cage. Each rhenium atom occupied the corner of the triangular prism and was bonded to one nitrogen atom of the pyridyl group of the tpt ligand, two butoxy groups and three carbonyl groups, maintaining a distorted octahedral geometry around it. The maximum and minimum rhenium-rhenium distances in the molecule were 13.5 and 3.4 Å respectively. The three pyridyl rings of tpt moiety were canted slightly ca. 15° from the plane containing the triazine ring. Some group of researchers have experienced difficulty to grow X-ray quality single crystals, in the case of metallomacromolecules containing more metal centers. See, e.g., Sun *et al.* (2000) *Inorg. Chem.* 39: 1344–1345; Sun & Lees (1999) *Inorg. Chem.* 38: 4181–4182; Constable & Schofield (1998) *Chem. Commun.* 403–404; and Manna, (1997) *J. Am. Chem. Soc.* 119: 11611–11619. In contrast, the synthetic strategy described above has led to the formation of single crystals of good quality. The electroneutrality of the cage Compounds 1–3 mitigated interference of the counter ions inside the cavity, which created problem in most of the sensor studies. The extraordinary affinity of oxygen with rhenium metal was emphasized in this synthetic approach by utilizing the oxo-bridges bearing hydrophobic long tails. The ¹H and ¹³C NMR spectral measurements and the FAB-MS data of the cage compounds were in agreement with the proposed structures.

2014-2015-2016-2017-2018-2019-2020-2021-2022-2023-2024-2025-2026-2027-2028-2029-2030

Interestingly the solubility of Compounds **1–3** has been improved enormously by changing the length of the alkyl moiety from butyl to octyl and then to dodecyl. The increase in the chain length of the alkoxo moiety increased the hydrophobicity of the cage, thereby increasing the solubility of the compound in organic solvents. Compounds **2** and **3** were 5 freely soluble in CH_2Cl_2 , $(\text{CH}_3)_2\text{CO}$ and other organic solvents compared to Compound **1**. Because of the greater solubility of Compounds **2** and **3**, the latter were used for further studies.

Compounds **2** and **3** displayed an identical CO stretching pattern in their infrared spectra which was similar to that observed for the previously reported compounds. See, e.g., 10 Benkstein *et al.* (1988) *Inorg. Chem.* 37: 5404–5405; Jiang *et al.* (1998) *Organometallics* 17: 173–181; and El-Sayed & Kaesz (1963) *Inorg. Chem.* 2: 158–162. The UV-Vis spectra of Compounds **2** and **3** in CH_2Cl_2 showed an intense high energy band at 243 nm and a broad low-energy band at 488 nm, respectively. In accord with the previous reports on related systems, the former absorption was assigned to the intraligand $\pi-\pi^*$ transition and the low energy absorption to a metal-to-ligand charge transfer (MLCT) transition. In addition, there 15 was a shoulder at about 265 nm, which may be assigned to another $\pi-\pi^*$ transition as suggested by Tapolsky *et al.* See, e.g., Tapolsky *et al.* (1991) *J. Phys. Chem.* 95: 1105–1112; Tapolsky *et al.* (1990) *Inorg. Chem.* 29: 2285–2297; and Tapolsky *et al.* (1989) *J. Phys. Chem.* 93: 3885–3887. The interesting feature that deserved further attention was 20 the observation of MLCT at comparatively large wavelength (488 nm), indicating the readily reducible nature of the ligand. The absorption spectra of Compounds **2** and **3** were recorded in a large number of solvents and they showed substantial solvatochromism; the λ_{\max}^{ab} value could be tuned over 125 nm with a change in the color of the solution from yellow to red with the change in polarity of the solvents (λ_{\max}^{ab} values for Compound **2** in DMSO and CCl_4 25 are 424 and 549 nm, respectively). See, e.g., Reichardt (1994) *Chem. Rev.* 94: 2319–2358.

Example 2. Synthesis and characterization of Compounds **4–9** having rectangular structures

In a typical preparation, a suspension containing a mixture of $\text{Re}_2(\text{CO})_{10}$ and the *N*-ligands in 10 ml aliphatic alcohol in a 30 ml Teflon flask was placed in an oven maintained at 30 120–160 °C and then cooled to 25 °C. The crystals were separated by filtration and the

solvent from the filtrate was removed by vacuum and the residue was redissolved in minimum quantity of CH_2Cl_2 and passed through a short silica gel column to get the pure product.

[$\{(CO)_3Re(\mu-\text{OC}_4\text{H}_9)_2Re(CO)_3\}_2(\mu\text{-pz})_2$] (Compound 4): Yield: 71%. IR (CH_2Cl_2): ν_{CO} 2024 (s), 2017 (sh, m), 1925 (m), 1903 (vs) cm^{-1} ; ^1H NMR (300 MHz, $(\text{CD}_3)_2\text{CO}$): δ 8.83 (s, 8 H, H^2), 4.44 (m, 8 H), 2.17 (m, 8 H), 1.48 (m, 8 H), 1.07 (t, $^3J = 7.4$ Hz, 12 H); ^{13}C NMR (75 MHz; $(\text{CD}_3)_2\text{CO}$): δ = 199.0, 198.2 (1:2, CO), 150.1 (C^2 , pyrazine), 82.9 (CH_2), 36.5 (CH_2), 19.0 (CH_2), 14.5 (CH_3); UV-VIS (CH_3CN): λ_{max} [nm] 452 (MLCT), 255, 261, 268 (LIG); Anal. for $\text{C}_{36}\text{H}_{44}\text{N}_4\text{O}_{16}\text{Re}_4$, Found (calcd): C, 28.09 (28.19); H, 2.85 (2.89); N, 3.73 (3.65); Mass (FAB, ^{187}Re): m/z = 1536 (M^+).

[$\{(CO)_3Re(\mu-\text{OC}_8\text{H}_{17})_2Re(CO)_3\}_2(\mu\text{-pz})_2$] (Compound 5): Yield: 73%. IR (CH_2Cl_2): ν_{CO} 2024 (s), 2018 (sh, m), 1924 (m), 1903 (vs) cm^{-1} ; ^1H NMR (300 MHz, $(\text{CD}_3)_2\text{CO}$): δ 8.83 (s, 8 H, H^2), 4.42 (m, 8 H), 2.20 (m, 8 H), 1.46 (m, 24 H), 1.35 (m, 16 H), 0.91 (t, $^3J = 6.9$ Hz, 12 H); ^{13}C NMR (75 MHz; $(\text{CD}_3)_2\text{CO}$): δ = 198.7, 197.1 (1:2, CO), 150.0 (C^2 , pyrazine), 83.1 (CH_2), 34.2 (CH_2), 32.5 (CH_2), 30.2 (CH_2), 29.9 (CH_2), 25.7 (CH_2), 23.3 (CH_2), 14.3 (CH_3); UV-VIS (CH_3CN): λ_{max} [nm] 459 (MLCT), 255, 261(LIG); Emission: λ_{max} [nm] 470; Anal. for $\text{C}_{52}\text{H}_{76}\text{N}_4\text{O}_{16}\text{Re}_4$, Found (calcd): C, 35.97 (35.53); H, 4.30 (4.36); N, 3.08 (3.18); Mass (FAB, ^{187}Re): m/z = 1760 (M^+).

[$\{(CO)_3Re(\mu-\text{OC}_4\text{H}_9)_2Re(CO)_3\}_2(\mu\text{-bpe})_2$] (Compound 6): Yield: 76%. IR (CH_2Cl_2): ν_{CO} 2020 (s), 2008 (m), 1909 (m), 1888 (vs) cm^{-1} ; ^1H NMR (300 MHz, $(\text{CD}_3)_2\text{CO}$): δ 8.46 (d, $^3J = 5.3$ Hz, 8 H, H^3), 7.63 (s, 4 H, vinyl), 7.59 (d, $^3J = 5.3$ Hz, 8 H, H^2), 4.41 (m, 8 H), 2.13 (m, 8 H), 1.49 (m, 8 H), 1.08 (t, $^3J = 7.4$ Hz, 12 H); ^{13}C NMR (125 MHz; $(\text{CD}_3)_2\text{CO}$): δ = 198.9, 198.5 (1:2, CO), 152.8 (C^3), 146.4 (C^1), 132.6 (vinyl), 124.0 (C^2), 82.5 (CH_2), 36.5 (CH_2), 19.1 (CH_2), 14.5 (CH_3); UV-VIS (CH_3CN): λ_{max} [nm] 398 (MLCT), 289 (LIG); Emission: λ_{max} [nm] 440, 454; Anal. for $\text{C}_{52}\text{H}_{56}\text{N}_4\text{O}_{16}\text{Re}_4$, Found (calcd): C, 35.98 (35.94); H, 3.27 (3.25); N, 3.33 (3.22); Mass (FAB, ^{187}Re): m/z = 1740 (M^+).

[$\{(CO)_3Re(\mu-\text{OC}_8\text{H}_{17})_2Re(CO)_3\}_2(\mu\text{-bpe})_2$] (Compound 7): Yield: 82%. IR (CH_2Cl_2): ν_{CO} 2020 (s), 2008 (m), 1909 (m), 1886 (vs) cm^{-1} ; ^1H NMR (300 MHz, $(\text{CD}_3)_2\text{CO}$): δ 8.46 (d, $^3J = 6.6$ Hz, 8 H, H^3), 7.62 (s, 4 H, (vinyl)), 7.57 (d, $^3J = 6.6$ Hz, 8 H, H^2), 4.39 (m, 8 H), 2.16 (m, 8 H), 1.47 (m, 24 H), 1.36 (m, 16 H), 0.92 (t, $^3J = 6.8$ Hz, 12 H);

¹³C NMR (75 MHz; (CD₃)₂CO): δ 199.0, 198.6 (1:2, CO), 152.1 (C³), 146.4 (C¹), 132.7 (vinyl), 124.1 (C³), 82.8 (CH₂), 34.4 (CH₂), 32.6 (CH₂), 30.4 (CH₂), 30.0 (CH₂), 26.0 (CH₂), 23.3 (CH₂), 14.4 (CH₃); UV-VIS (CH₃CN): λ_{max} [nm] 398 (MLCT), 289 (LIG); Emission: λ_{max} [nm] 460; Anal. for C₆₈H₈₈N₄O₁₆Re₄, Found (calcd): C, 41.58 (41.62); H, 4.47 (4.52); N, 2.85 (2.86); Mass (FAB, ¹⁸⁷Re): *m/z* = 1964 (M⁺).

5 [{{(CO)₃Re(μ-OC₄H₉)₂Re(CO)₃}₂(μ-bpeb)₂] (Compound 8): Yield: 78%. IR (CH₂Cl₂): ν_{CO} 2019 (s), 2005 (m), 1905 (m), 1884 (vs) cm⁻¹; ¹H NMR (300 MHz, (CD₃)₂CO): δ 8.36 (d, ³J = 6.5 Hz, 8 H, (pyridyl) H³), 7.54 (d, ³J = 16.4 Hz, 4 H, (vinyl) H²), 7.47 (d, ³J = 6.5 Hz, 8 H, (pyridyl) H²), 7.38 (s, 8 H (phenyl)), 7.18 (d, ³J = 16.4 Hz, 4 H 10 (vinyl) H¹), 4.40 (m, 8 H), 2.13 (m, 8 H), 1.49 (m, 8 H), 1.08 (t, ³J = 7.3 Hz, 12 H); UV-VIS (CH₃CN): λ_{max} [nm] 423 (MLCT), 269, 364 (LIG); Emission: λ_{max} [nm] 474; Anal. for C₆₈H₈₈N₄O₁₆Re₄, Found (calcd): C, 42.37 (42.05); H, 3.42 (3.53); N, 2.92 (2.88); Mass (FAB, ¹⁸⁷Re): *m/z* = 1944 (M⁺).

15 [{{(CO)₃Re(μ-OC₈H₁₇)₂Re(CO)₃}₂(μ-bpeb)₂] (Compound 9): Yield: 84%. IR (CH₂Cl₂): ν_{CO} 2020 (s), 2006 (m), 1906 (m), 1883 (vs) cm⁻¹; ¹H NMR (300 MHz, (CD₃)₂CO): δ 8.36 (d, ³J = 6.6 Hz, 8 H, (pyridyl) H³), 7.53 (d, ³J = 16.4 Hz, 4 H, (vinyl) H²), 7.46 (d, ³J = 6.6 Hz, 8 H, (pyridyl) H²), 7.38 (s, 8 H, (phenyl)), 7.18 (d, ³J = 16.4 Hz, 4 H, (vinyl) H¹), 4.39 (m, 8 H), 2.15 (m, 8 H), 1.47 (m, 24 H), 1.37 (m, 16 H), 0.92 (t, ³J = 6.8 Hz, 12 H); ¹³C NMR (75 MHz; (CD₃)₂CO): δ 199.1, 198.7 (1:2, CO), 152.4 (pyridyl) C³, 148.0 (pyridyl) C¹, 137.3 (phenyl) C¹, 136.0 (vinyl) C², 128.5 (phenyl) C², 125.9 (vinyl) C¹, 123.2 (pyridyl) C², 82.8 (CH₂), 34.4 (CH₂), 32.6 (CH₂), 26.0 (CH₂), 23.3 (CH₂), 14.4 (CH₃); UV-VIS (CH₃CN): λ_{max} [nm] 422 (MLCT), 235, 285, 370 (LIG); Emission: λ_{max} [nm] 474, 490; Anal. for C₈₄H₁₀₀N₄O₁₆Re₄, Found (calcd): C, 46.07 (46.57); H, 4.42 (4.65); N, 1.89 (2.59); Mass (FAB, ¹⁸⁷Re): *m/z* = 2168 (M⁺).

25 Crystallographic data: [C₆₈H₈₈N₄O₁₆Re₄] (Compound 8): *M* = 1942.06, *T* = 150(1) K, monoclinic, Space group = P2₁/n, *a* = 9.2304(1), *b* = 23.5898(1), *c* = 15.9339(2) Å, β = 98.796(1)°, *V* = 3428.69(6) Å³, *Z* = 2, *D_c* = 1.881 g/cm³, μ = 7.106 mm⁻¹, 24951 reflections collected, 7796 independent reflections (*R_{int}* = 0.0420), refinement method: full-matrix least-squares on *F*², Final *R* indices [*I* > 2σ(*I*)]: *R*₁ = 0.0379, *wR*₂ = 0.0658, *R* indices (all data): *R*₁ = 0.0512, *wR*₂ = 0.0699, Largest diff. Peak and hole: 1.187 and -0.786 e Å⁻³. X-ray quality 30

crystals were obtained by solvothermal means and the X-ray diffraction study was carried out for Compound **8**. The ORTEP diagram of Compound **8** revealed a rectangular architecture, where two planar bpeb ligands coordinated to four rhenium atoms, which were connected by four butoxy bridges thereby forming a molecular rectangle. Each rhenium atom occupied the corner of the rectangle and was bonded to one nitrogen atom of the pyridyl group of the bpeb ligand, two butoxy groups and three carbonyl groups. In each bridging ligands (bpeb), the two pyridyl groups and the central aromatic ring were oriented in the same plane.

The IR spectra of Compounds **4–9** showed a gradual shift in the carbonyl stretching frequencies, when the ligand was changed from bpeb (bpe) to pz. See, e.g., El-Sayed & Kaesz (1963) *Inorg. Chem.* 2: 158; and Jiang *et al.* (1998) *Organometallics* 17: 173. This indicated that among the three ligands used, the coordinating ability of bpeb and bpe was comparable but stronger than pz. The electronic absorption spectral studies of Compounds **4–9** revealed the existence of two types of bands, one in the UV and the other in the visible region. In a broad way, the higher energy features were assigned to the ligand ($\pi-\pi^*$) based transition, and the lower energy absorption was assigned to the metal-to-ligand (bridging) charge transfer (MLCT) transition. See, e.g., Giordano & Wrighton (1979) *J. Am. Chem. Soc.* 101: 2888; Kalyanasundaram *Photochemistry of polypyridine and porphyrin complexes*, Academic Press, London, 1992; and Meyer (1986) *Pure Appl. Chem.* 58: 1193. The higher energy absorption ($\pi-\pi^*$) was always intense, about four fold stronger than the MLCT transition. A red shift of 61 nm (from 398 nm to 459 nm) was felt with the MLCT absorption maxima of these compounds, on changing the ligand from bpe to pz. The observation that the more easily reducible ligands yielded complexes exhibiting lower energy absorption, was in agreement with the results of Wrighton *et al.* (*supra*). With the molecular squares, a change of ligand from bpe to pz shifted the lower energy λ_{\max} from 358 nm to 396 nm (Slone *et al.* (1996) *Inorg. Chem.* 35: 4096). Thus the alkoxy bridges facilitate the $\text{Re} \rightarrow \text{L}$ charge transfer. It is interesting to note that the (MLCT) band of Compounds **4** and **5** was highly sensitive to the change in the polarity of the solvent and exhibited solvatochromism having a shift in the λ_{\max} to the tune of 100 nm when the solvent was varied from DMSO to CCl_4 . Excitation of the complexes near MLCT absorption resulted in moderate emission in the range 440 to 490 nm in CH_3CN and CH_2Cl_2 . However, the free ligands also showed emission in the above region. Since both the free ligands and rectangles exhibited emissions

around the same region, the observed emission for the complexes may therefore be originated from the MLCT band involving primarily the bridging ligands. The excited state lifetimes of these rectangles have been measured and are in the range of 10 to 15 ns at room temperature.

The measured cyclic voltammetric data showed that each of the complexes studied here displays two or three reduction waves and one to four oxidation waves. The first reduction wave in the range -0.73 to -1.28 V can be assigned to the first reduction of the bridging ligand, L/L⁻. See, e.g., Worl *et al.* (1991) *J. Chem. Soc., Dalton Trans.* 849; Lin *et al.* (1992) *Inorg. Chem.* 31: 4346; Stor *et al.* (1995) *Organometallics* 14: 1115; and Moya *et al.* (1994) *Inorg. Chem.* 33:2341. The second reduction observed with the complexes containing bpe and bpeb at -1.26 V and -1.28 V may be assigned to the second reduction of the ligand, L/L²⁻. The reduction wave observed in the range of -1.35 to -1.50 V in the case of complexes containing bpe and pz can be assigned to the reduction of metal, Re⁺/Re⁰ (See Lin, *supra*; and Moya *supra*). The oxidation peaks observed in the range 1.00–1.65 V may be attributed to the oxidation of four metal centers present in the rectangle. As the alkoxy bridge remains as a good electron donor in the present system it is not able to show any redox reaction in the potential range -2.00 to 2.00 V.

Example 3. Synthesis characterization of Compounds 10-12 having rectangular structures

In a typical preparation, a suspension containing a mixture of Re₂(CO)₁₀ (0.199 mmol, 130 mg) and the 4,4'-bipyridine (0.205 mmol, 32 mg) in 10 mL aliphatic alcohol in a 30 mL Teflon flask was placed in an oven maintained at 160 °C and then cooled to 25 °C. The crystals were separated by filtration and the solvent from the filtrate was removed by vacuum and the residue was redissolved in minimum quantity of CH₂Cl₂ and passed through a short silica gel column to get the pure product. Yield: Compound 10, 84%; Compound 11, 86%; Compound 12, 87%.

Compound 10: IR (CH₂Cl₂): ν_{CO} 2022 (s), 2010 (m), 1912 (m), 1890 (vs) cm⁻¹; ¹H NMR (300 MHz, (CD₃)₂CO): δ 8.65 (d, ³J = 6.6 Hz, 8 H, H³), 7.84 (d, ³J = 6.6 Hz, 8 H, H²), 4.45 (m, 8 H), 2.17 (m, 8 H), 1.51 (m, 8 H), 1.10 (t, ³J = 7.4 Hz, 12 H); ¹³C NMR (75 MHz, (CD₃)₂CO): δ 198.9, 198.4 (1:2, CO), 153.6 (C³), 146.2 (C¹), 124.2 (C²), 82.7 (CH₂), 36.7 (CH₂), 19.2 (CH₂), 14.6 (CH₃); UV-VIS (CH₃CN): λ_{max} [nm] 384 (MLCT), 249 (LIG);

Emission: λ_{\max} [nm] 666; Anal. for $C_{48}H_{52}N_4O_{16}Re_4$, Found (calcd): C, 34.20 (34.20); H, 3.02 (3.11); N, 3.36 (3.32); Mass (FAB, ^{187}Re): m/z = 1688 (M^+).

Compound **11**: IR (CH_2Cl_2): ν_{CO} 2022 (s), 2009 (m), 1912 (m), 1890 (vs) cm^{-1} ; 1H NMR (300 MHz, $(CD_3)_2CO$): δ 8.65 (d, 3J = 6.7 Hz, 8 H, H^3), 7.83 (d, 3J = 6.7 Hz, 8 H, H^2), 4.44 (m, 8 H), 2.20 (m, 8 H), 1.49 (m, 24 H), 1.35 (m, 16 H), 0.92 (t, 3J = 6.9 Hz, 12 H); ^{13}C NMR (75 MHz; $(CD_3)_2CO$): δ = 198.8, 198.3 (1:2, CO), 153.5 (C^3), 146.1(C^1), 124.1(C^2), 82.8 (CH_2), 34.4 (CH_2), 32.5 (2 CH_2), 30.3 (CH_2), 25.8 (CH_2), 23.3 (CH_2), 14.5 (CH_3); UV-VIS (CH_3CN): λ_{\max} [nm] 398 (MLCT), 248 (LIG); Emission: λ_{\max} [nm] 666; Anal. for $C_{64}H_{84}N_4O_{16}Re_4$, Found (calcd): C, 41.12 (40.24); H, 4.75 (4.43); N, 2.65 (2.93); Mass (FAB, ^{187}Re): m/z = 1912 (M^+).

Compound **12**: IR (CH_2Cl_2): ν_{CO} 2022 (s), 2010 (m), 1912 (m), 1890 (vs) cm^{-1} ; 1H NMR (300 MHz, $(CD_3)_2CO$): δ 8.63 (d, 3J = 6.5 Hz, 8 H, H^3), 7.80 (d, 3J = 6.5 Hz, 8 H, H^2), 4.43 (m, 8 H), 2.19 (m, 8 H), 1.48 (m, 24 H), 1.30 (m, 48 H), 0.89 (t, 3J = 6.5 Hz, 12 H); ^{13}C NMR (75 MHz; $(CD_3)_2CO$): δ = 199.0, 198.3 (1:2, CO), 153.5 (C^3), 146.0 (C^1), 124.0 (C^2), 82.9 (CH_2), 34.3 (CH_2), 32.6 (CH_2), 30.3 (3 CH_2); 30.0 (2 CH_2); 25.8 (2 CH_2); 23.3 (CH_2); 14.4 (CH_3); UV-VIS (CH_3CN): λ_{\max} [nm] 382 (MLCT), 247 (LIG); Emission: λ_{\max} [nm] 666; Anal. for $C_{80}H_{116}N_4O_{16}Re_4$, Found (calcd): C, 46.62 (45.01); H, 5.96 (5.48); N, 2.26 (2.62); Mass (FAB, ^{187}Re): m/z = 2136 (M^+).

Crystallographic data: [$C_{48}H_{52}N_4O_{16}Re_4$] Compound **10**: M = 1685.74, T = 295(2) K, monoclinic, Space group = $P2_1/n$, a = 9.280(2), b = 18.613(2), c = 15.189(2) Å, β = 93.90(2)°, V = 2617.6(7) Å³, Z = 2, D_c = 2.139 Mg/m³, μ = 9.290 mm⁻¹, 4602 reflections collected, 4602 independent reflections, refinement method: full-matrix least-squares on F^2 , Final R indices [$I > 2\sigma (I)$]: R_1 = 0.0319, wR_2 = 0.0743, R indices (all data): R_1 = 0.0639, wR_2 = 0.0814, Largest diff. Peak and hole: 1.070 and -1.047 e Å⁻³.

The ORTEP diagram of Compound **10** revealed a rectangular architecture, where two planar bpy ligands coordinated to four rhenium atoms, which were connected by four butoxy bridges thereby forming a molecular rectangle. Each rhenium atom occupied the corner of the rectangle and was bonded to one nitrogen atom of the pyridyl group of the bpy ligand, two butoxy groups and three carbonyl groups. The four butoxy groups were oriented in such a way that they were away from plane bisecting the four Re atoms and two bipyridine

ligands. The IR spectra of Compounds **10–12** showed an identical CO stretching pattern similar to the previous reports. The ^1H and ^{13}C NMR spectral studies and the FAB-MS data of Compounds **10–12** were in agreement with the proposed structures.

The cyclic voltammetric data showed that the Compound **12** displayed two reduction waves and four oxidation waves. The first reduction wave at -1.28 V can be assigned to the reduction of the bridging ligand, $(\text{bpy})/(\text{bpy})^-$ and the second one at -1.50 V to the reduction of metal, Re^+/Re^0 . The oxidation peaks observed in the range $1.00\text{--}1.65\text{ V}$ may be attributed to the oxidation of four metal centers present in the rectangle. The absorption spectrum of Compound **12** showed two peaks in CH_3CN at 250 and 380 nm and they corresponded to the ligand centered (LC) and metal-to-ligand charge transfer (MLCT) transitions, respectively. Addition of water blue shifts the λ_{\max} of MLCT to 370 nm and increased the absorption intensity. The blue shift in λ_{\max} was in accordance with negative solvatochromism and the increase in the intensity indicated aggregation of Compound **12**.

Example 4. Luminescence enhancement via aggregation in Compounds **10–12**

The molecular rectangles Compounds **10–12** contain long alkyl chains. Surfactants carrying long alkyl chains undergo self-aggregation in aqueous medium and if such aggregation takes place in the presence of metal ions, the term metalloaggregates is used. See, e.g., Tonellato (1998) *Pure & Appl. Chem.* 70: 1961; and Hamilton Ed. *Perspectives in Supramolecular Chemistry: Supramolecular control of Structure and Reactivity*; John Wiley & Sons, New York, 1996. A substantial blue shift in the wavelength of emission maximum ($\lambda_{\max}^{\text{em}}$) from 666 to 602 nm and large enhancement in the emission intensity (a 80-fold increased i.e., from Compound **12** in CH_3CN to 227 in 90% H_2O –10% CH_3CN) and lifetime has been observed on addition of water to Compound **12** in CH_3CN (Table 1) (The concentration of Compound **12** is $1\text{ }\mu\text{M}$). A similar increase in emission quantum yield was also obtained and the values in CH_3CN and in 90% H_2O –10% CH_3CN are 0.77×10^{-4} and 16.3×10^{-4} , respectively. The change of emission intensity with the change of solvent composition was determined and the lifetime and $\lambda_{\max}^{\text{em}}$ data was collected as shown in Table 1. The enhancement in emission was marginal with rectangles containing butyl and octyl groups but substantial with dodecyl-containing compounds. The observed blue shift in

$\lambda_{\max}^{\text{em}}$ may be related to the "luminescence rigidochromic effect" that has been recognized for a number of metal carbonyl complexes exhibiting MLCT emission. See, e.g., Kotch *et al.* (1993) *Inorg. Chem.* 32: 2570; and Lees (1987) *Chem. Rev.* 87: 711. In order to rationalize the rigidochromic effect it is useful to compare the electronic absorption and emission results. Compared to the emission energies, the absorption maximum showed relatively small dependence upon variation of solvent composition. The different behavior of absorption and emission spectral changes can be understood from the different lifetimes of $^1\text{MLCT}$ and $^3\text{MLCT}$ states. The absorption and emission spectral results suggested that the relatively long-lived $^3\text{MLCT}$ was most affected by the environment changes as it was more susceptible to alterations in dipolar interactions with the molecules present in the medium. In order to confirm the aggregate formation the concentration was measured dependence of emission intensity. Emission intensity increases with an increase in the concentration of the rectangle reached maximum at 2.0×10^{-5} M and remained constant afterwards. Thus the aggregation process was completed at 2.0×10^{-5} M and this value can be taken as critical micellar concentration (CMC).

It is worthwhile to compare these unexpected observations with the results observed by Demas and co-workers (Reitz *et al.* (1988) *J. Am. Chem. Soc.* 110: 5051) on monometallic Re(I) carbonyl complexes. These authors discovered the remarkable phenomenon that the electronically passive alkyl chains perturbed the emission of Re(I) complex dramatically. They attributed this perturbation to an intramolecular fold back of the chain onto the bipyridine ligand. This fold back perturbed the solvent environment around the excited portion of the complex and altered the excited-state properties. However in a subsequent report (Sacksteder *et al.* (1993) *J. Am. Chem. Soc.* 115: 8230), they have concluded that the emission enhancement was due to isonitrile impurities. If the intramolecular fold back of the alkyl chain was the major reason for the luminescence enhancement in the present study, it should be felt even in pure solvents i.e., in CH₃CN. But in the case of Compounds **10–12**, the emission enhancement was observed only in the presence of water and improved with the increase in the water content of the medium. The possible explanation for this emission enhancement was the self-aggregation of molecules carrying long alkyl chains. It has been well established, even in the case of Re(I) complexes, that the emission enhancement is observed when the system is rigid. Thus the emission enhancement in the aqueous medium

is due to the rigidity of the molecule resulting from the self-aggregation of the rectangle. The major reason for the poor emission of some metal complexes is the dominance of nonradiative over radiative deactivation of the molecule in the excited state. See, e.g., Turro *Modern Molecular Photochemistry*; Benjamin/Cummings, 1991; and Chen & Meyer (1998)

5 *Chem. Rev.* 98: 1439. The introduction of rigidity either in the molecule or in the medium suppresses the nonradiative transition resulting in luminescence enhancement. To confirm this, the emission spectra of the rectangle in the presence of anionic and cationic surfactants were recorded. The large emission was observed in the presence of low surfactant concentrations but increase in surfactant concentrations led to decrease in emission intensity.

10 To realize the role of added surfactants here, the absorption spectrum of Compound **12** at different concentration of cetyltrimethylammonium bromide (CTAB) was recorded. It is interesting to note that initial addition of CTAB increased the absorption intensity of Compound **12** but the spectrum became closer to the one observed at pure CH₃CN at high CTAB concentrations. Thus, aggregation was complete even in the absence of surfactants and therefore addition of surfactants disturbed the aggregation due to the competitive hydrophobic interaction of the surfactant with the hydrophobic alkyl group of the rectangle.

15 In order to realize the molecular recognition capability of this luminescent rectangle as host, the reaction of Compound **12** with methyl viologen (MV²⁺) was studied by luminescence quenching technique. The quenching reaction was efficient and the quenching rate constant, k_q, value was $1 \times 10^9 \text{ M}^{-1}\text{s}^{-1}$ (calculated from Stern-Volmer plot), close to diffusion controlled rate in 90% H₂O–10% CH₃CN(v/v). The addition of 1,4-dicyanobenzene to Compound **12** in 50% H₂O–50% CH₃CN(v/v) shifted the $\lambda_{\max}^{\text{em}}$ from 613 nm to 603 nm and increased the luminescence intensity implying binding. Thus Compounds **10–12** can be used as luminescent hosts in host-guest studies.

25

Example 5. Synthesis and characterization of Compounds **13–15** having tetragonal prismatic structures

30 Solvothermal synthesis of tetragonal prismatic cages, [{}(CO)₃Re(μ_2 -OR)₂Re(CO)₃)₄(μ_4 -tpeb)₂], (**13**, R = C₈H₁₇; **14**, R = C₁₂H₂₅; **15**, R = C₇H₇) was carried out using Re₂(CO)₁₀ and the ligand tpeb in the alcohol of interest in the ratio 2:1. Prismatic cages **13–15** are the first example of M₈L₂L₈ type supramolecules possessing eight

octahedral Re(I) centers and two different kinds of ligands, characterized crystallographically having molecular weight more than 4000 and unique having eighteen aromatic rings.

Compound 13. Anal. Calcd for $C_{156}H_{172}N_8O_{32}Re_8$: C, 45.03; H, 4.17; N, 2.69. Found: C, 45.20; H, 4.66; N, 2.33%.

Compound 14. Calcd for $C_{188}H_{236}N_8O_{32}Re_8$: C, 48.99; H, 5.16; N, 2.43. Found: C, 48.95; H, 5.58; N, 2.02%.

Compound 15. Calcd for $C_{162}H_{108}N_8O_{32}Re_8$: C, 46.68; H, 2.61; N, 2.69. Found: C, 46.52; H, 2.61; N, 2.67%.

Compound 15 has been characterized structurally and spectroscopically. Single crystal X-ray crystallographic study of the dark-red crystal of Compound 15 established the stoichiometry, $C_{148}H_{92}N_8O_{32}Re_8(C_6H_5CH_3)_2$. The ORTEP diagram of Compound 15 is shown below and the core geometry of Compound 15 consists of a heavy atom prism made up of eight Re atoms.

The molecular structure of Compound 15 reveals prismatic cage architecture where two planar tpeb ligands coordinate to eight Re atoms which are themselves connected to eight benzyloxy bridges thereby forming a tetragonal prismatic cage. Each Re is bonded to one tpeb nitrogen, two benzyloxy oxygens and three terminal carbonyls. Compound 15 is a unique octanuclear rectangular prismatic cage and the lateral dimension is ~ 20 (Re1—Re3A) \times 10 (Re1—Re4) \times 4 (Re1—Re2) Å. It can also be viewed as a tetragonal prism. Each corner of the rectangular prismatic cage is occupied by $\{(CO)_3Re(\mu_2-OCH_2C_6H_5)_2Re(CO)_3\}$ moiety where the Re1 and Re2 look like the head and tail of a flying eagle with two benzyloxy wings. Compound 15 consists of eighteen aromatic rings where ten aromatic rings of the two tpeb moieties are oriented in the plane of the molecule with an effective $\pi-\pi$ stacking and the remaining eight aromatic rings of the benzyloxy moieties are almost perpendicular to the molecular plane.

Compounds 13–15 displayed CO stretching frequencies in its infrared spectrum similar to that observed for previously reported compounds (e.g., Manimaran *et al.* (2001). *Eur. J. Inorg. Chem.* 633). The 1H and ^{13}C NMR spectra exhibit signals for the presence of tpeb ligand, alkyloxy, benzyloxy moieties and CO groups. The prismatic cages show a sharp absorption at 317 nm and a shoulder at 365 nm irrespective of the polarity of the medium. The sharp intense absorption at 317 nm may be assigned to the $\pi-\pi^*$ transition of the highly

conjugated bridging ligand tpeb and the shoulder at 365 nm to the MLCT transition $\text{Re} \rightarrow$ tpeb in line with the previous reports (e.g., Chen & Meyer (1998) *J. Chem. Rev.* 98: 1439 and references therein). Since some Re(I) containing rectangles are emissive (see Rajendran *et al.* (2000) *Inorg. Chem.* 39: 2016), the emission spectrum of Compounds **13–15** in THF,
5 DMF and pyridine were recorded and surprisingly, Compounds **13** and **14** were weakly emissive at room temperature when pyridine was used as solvent. The emission maximum was at 648 nm for Compound **13** and 624 nm for Compound **14** and no emission was observed for Compound **15**. However, the emission is improved at 77K and the emission maximum is blue shifted to 628 nm. The bi-layer tetragonal supramolecules separated by ~ 4
10 Å was weakly emissive due to the π - π stacking of the acetylene groups. When π -acceptor ligands such as pyridine and methyl phenyl sulphide were added, they interacted with the acetylene groups, extended conjugation and made the supramolecule more emissive. The excited state lifetime of Compound **13** and Compound **14** in pyridine at room temperature were both 10 ns. It is worthwhile to recall that the ligand tpeb itself was highly emissive and the emission maximum is at 770 nm. This on complexation was blue shifted to the tune of
15 146 nm.

As the supramolecules are emissive, use of this property for molecular recognition was studied. The emission spectrum of Compound **13** in pyridine in the absence and presence of different concentration of 1,4-dicyanobenzene were determined. The increase in the emission intensity of Compounds **13** and **14** with the increase in the concentration of 1,4-dicyanobenzene indicates that binding took place between Compounds **13** and **14** and 1,4-dicyanobenzene. The binding constants calculated are in the range of 120 M^{-1} for Compound **13** and 312 M^{-1} for Compound **14**. Similar trend has also been observed when methyl phenyl sulphide was used as a guest but the binding constants were below 4 M^{-1} .
20 Since Compounds **13–15** are not emissive in THF and DMF solvents, the quenching of these cages with pyrene as photosensitizer was studied. The absorption spectra of pyrene in the absence and presence of Compounds **13–15** were recorded and interestingly found an increase in the absorbance of pyrene due to complex formation. Using Benesi-Hildebrand method (e.g., Murakami *et al.* (1988) *J. Chem. Soc. Perkin Trans. 1*, 1289; and Benesi &
25 Hildebrand (1949) *J. Am. Chem. Soc.* 71: 2703), the binding constants were found to be in the range of $2.2 - 9.2 \times 10^4 \text{ M}^{-1}$. The quenching of emission intensity of pyrene with the
30

change of the concentration of Compound **15** was also determined. Using the luminescence quenching data, a Stern-Volmer plot (e.g., Rajendran *et al.* (1997) *J. Chem. Soc. Faraday Trans.* 93: 3155) was plotted, and the plot was linear at low concentration of Compounds **13–15** giving the quenching rate constant value $2.1\text{--}2.6 \times 10^{13} \text{ M}^{-1}\text{s}^{-1}$ and at high concentrations deviation from the linearity has been observed. This study indicates strong interaction between pyrene and prismatic cages **13–15**. Further, in order to tune the luminescence property of Compound **13–15**, the emission spectra of these prismatic cages in THF-H₂O media were recorded. Interestingly, in 80% and 90% water, the emission emerge at 655 and 664 nm for Compound **13**, 645 and 666 nm for Compound **14**, and 667 and 664 nm for Compound **15** respectively. As discussed previously, it has been observed the molecular aggregation and emission enhancement of alkoxy-bridged Re(I) based molecular rectangles in the presence of water.

In conclusion, the self-assembly of eighteen components into an tetragonal rectangular prismatic supramolecule bearing octahedral Re centers was accomplished in one pot synthesis. It is the first neutral luminescent Re-based supramolecule that is structurally characterized. The presence of lengthy alkyl increases the solubility of these supramolecules dramatically. The luminescence properties and host-guest interaction studies make these tetragonal prismatic cages interesting species.

Table 1 Emission Wavelength, Intensity and Lifetime of Compound 12 in Various CH₃CN:H₂O(v/v) Mixtures

solvent composition		$\lambda_{\text{max}}^{\text{em}}$ (nm)	Intensity	τ (ns)
no	%CH ₃ CN	%H ₂ O		
1	10	90	602	227
2	20	80	604	166
3	30	70	611	136
4	40	60	612	133
5	50	50	613	124
6	60	40	613	74
7	70	30	611	72
8	80	20	612	59
9	90	10	634	12
10	100	00	666	3

OTHER EMBODIMENTS

All of the features disclosed in this specification may be combined in any combination. Each feature disclosed in this specification may be replaced by an alternative feature serving the same, equivalent, or similar purpose. Thus, unless expressly stated otherwise, each feature disclosed is only an example of a generic series of equivalent or similar features.

From the above description, one skilled in the art can easily ascertain the essential characteristics of the present invention, and without departing from the spirit and scope thereof, can make various changes and modifications of the invention to adapt it to various usages and conditions. Accordingly, other embodiments are also within the scope of the following claims.